doi.org/10.36721/PJPS.2024.37.6.REG.1351-1363.1

Berberine inhibits the glycolysis and proliferation of hepatocellular carcinoma cells by down-regulating HIF-1α

Lin Chen and Yeqin Mao*
Department of Pharmacy, the First Affiliated Hospital of Soochow University, Suzhou City, Jiangsu Province, China

Abstract: Berberine (BBR), an isoquinoline alkaloid abundant in *Coptis chinensis*, exhibits anti-tumor and hypoglycemic properties. The regulation of tumor cell homeostasis and metabolism is greatly influenced by Hypoxia-inducible factor-1α (HIF-1α). This research aims to elucidate whether BBR inhibits the progression of hepatocellular carcinoma (HCC) by modulating HIF-1α expression. Simulating the tumor hypoxic microenvironment *in vitro* by $CoCl_2$ addition to induce the HIF-1α expression. The optimal concentration of BBR and $CoCl_2$ were screened by CCK-8 assay. Clone formation, wound healing, EDU staining, Transwell assay, and flow cytometry evaluated the malignant biological behavior of HepG2 cells. RT-qPCR and Western blot assessed HIF-1α and glycolysis-related protein levels. Finally, the influence of BBR *in vivo* was investigated by a xenograft tumor model in nude mice. After exposure to 100 μmol/L BBR, the proliferation, migration and invasion of HepG2 cells were reduced, along with apoptosis was increased, while the levels of glycolysis-related proteins were decreased (P<0.05). 100 μmol/L $CoCl_2$ treatment increased the level of HIF-1α, promoted the malignant progression of HCC and attenuated the anti-tumor effect of BBR. Additionally, BBR inhibited tumor growth in nude mice. In conclusion, BBR exerts antitumor effects through upregulating HIF-1α and could be used as a therapeutic agent for HCC.

Keywords: Berberine, HIF-1α, hepatocellular carcinoma, glycolysis, proliferation

Submitted on 21-08-2024 – Revised on 02-10-2024 – Accepted on 17-10-2024

INTRODUCTION

Liver cancer is the fifth most common cancer in the world and its incidence is increasing every year (Chen *et al.*, 2023). According to statistics, in 2020, there were 900,000 new cases of liver cancer, with over 800,000 recorded deaths worldwide, projections indicate that the annual incidence of liver cancer will rise by 55.0% from 2020 to 2040 (Sung *et al.*, 2021, Rumgay *et al.*, 2022). Hepatocellular carcinoma (HCC) is a major histologic subtype of primary liver cancer (Sarcognato *et al.*, 2021, Cogliati *et al.*, 2023). Among these liver cancers, HCC stands out as the most prevalent, making up about 90% of cases and ranking fourth in cancer-related deaths worldwide (Kim *et al.*, 2020). Surgery is the first choice of HCC patients, but the majority of patients present to the clinic at an intermediate to advanced stage, when hepatectomy or radiofrequency ablation is no longer possible (Liu *et al.*, 2021). Asian countries have a low five-year survival rate of 18.1% for HCC patients, largely attributed to the absence of effective treatments (Hassanipour *et al.*, 2020). Hence, it is essential to clarify the molecular mechanisms that underlie the progression of HCC and to investigate innovative and effective treatment options.

The process of cancer development is intricate, characterized by continuous interactions between cancer cells and the tumor microenvironment (TME)(Hinshaw *et al.*, 2019, Xiao *et al.*, 2021). TME is marked by hypoxia, with hypoxia-inducible factor-1α (HIF-1α) playing a crucial role in maintaining cellular oxygen levels and metabolism (Kheshtchin *et al.*, 2022). HIF-1α mediates the up-regulation of glucose transporter proteins and glycolytic enzymes, increases the energy supply for glycolysis, and promotes the adaptation of cancer cells to a hypoxic environment (Kierans *et al.*, 2021). Furthermore, HIF-1α is abundantly present in HCC cells and correlates with unfavorable patient outcomes (Feng *et al.*, 2020, Huang *et al.*, 2021). Based on the importance of HIF-1α, there is potential for treating HCC with drugs that target HIF-1α inhibition.

Extensive research has revealed that certain natural medicines, especially Chinese herbs (including *Coptis chinensis*, *Scutellaria baicalensis* Georgi and *Curcuma longa* L.), have significant anti-tumor functions, and have multiple targets, relatively mild effects, and few side effects (Wang *et al.*, 2021, Sun *et al.*, 2022). As an isoquinoline alkaloid obtained from the traditional Chinese medicine *Coptis chinensis*, Berberine (BBR) is used clinically for the management of gastroenteritis, cardiac arrhythmia, and other diseases (Song *et al.*, 2020, Zhang *et al.*, 2020a). BBR has a variety of pharmacological effects and has broad application prospects in anti-cancer, anti-hypertension, hypoglycemia and hypolipidemia, etc. (Och *et al.*, 2020, Xiong *et al.*, 2022). Research indicates that BBR enhances the responsiveness of ovarian cancer cells to cisplatin and has the potential to improve the efficacy of anticancer medications (Liu *et al.*, 2019). Additionally, BBR inhibits proliferation migration and invasion of gastric cancer cells and induces G0/G1 cell blockade (Xu *et al.*, 2022).

**Corresponding author:* e-mail: wenqia05843@163.com

Not only that, BBR can down-regulate HIF-1α in the hypoxic microenvironment, and hinder the proliferation and metastasis of breast cancer cells (Sun *et al.*, 2023). However, it remains unknown whether BBR hinders the malignant development of HCC through regulating HIF-1α expression.

Thus, we postulated that BBR might suppress the progression of HCC by down-regulating HIF-1α. Based on this hypothesis, HepG2 cells were induced by $CoCl_2$ to mimic the tumor hypoxic microenvironment *in vitro*, to increase HIF-1α level. The impacts of BBR on the progression and glycolysis of HepG2 cells were investigated by studying the regulation of HIF-1α. This study sought to elucidate the influence of BBR on HCC and its specific action mechanism, and to offer a new insight for the clinical use of BBR in treating HCC.

MATERIALS AND METHODS

Cell culture and processing

Human hepatocellular carcinoma cells HepG2 (CL-0103, STR was correctly identified) were purchased from Pricella Biotechnology Co., Ltd (Wuhan, Hubei, China). The mixture of DMEM medium (10566016, Gibco, Grand Island, NY, USA), 10% fetal bovine serum (F0193, Sigma-Aldrich, St. Louis, MO, USA) and 1% penicillin/streptomycin (15140122, Gibco) was used for incubation. The incubation temperature was 37°C with 5% CO_2. 1: 3 digestion was passaged after the cells reached 80% confluence.

Based on previous reports (Zhang *et al.*, 2020b, Jampasri *et al.*, 2022), in the experiments of BBR (HY-N0716, Med Chem Express, Monmouth Junction, NJ, USA) and $CoCl_2$ (409332, Sigma-Aldrich) concentration gradients for the detection of HepG2 cell viability, the concentrations of both BBR and $CoCl_2$ were 0, 50, 100 or 200 μmol/L. In the subsequent HepG2 cell biological characterization assay, the BBR and $CoCl_2$ groups were exposed to 100μmol/L BBR or $CoCl_2$ for 48 h, respectively. In the BBR+$CoCl_2$ group, the HepG2 cells were first intervened with $CoCl_2$ for 1 h, subsequently co-treated with BBR for 48 h.

CCK-8 assay

HepG2 cells were inoculated into 96-well plates (1.5×10^4 cells/well) and after the cell adhesion, the original medium was discarded and exchanged for 200μL of medium containing varying doses of BBR or $CoCl_2$. Following 24, 48 or 72 h of culturing, 20μL of CCK-8 reagent (C0038, Beyotime, Shanghai, China) was introduced into every well. Following a 2-hour incubation, the OD_{450} values of the cells were determined by using an enzyme marker (1410101, Thermo Fisher Scientific, Waltham, MA, USA).

Clone formation assay

HepG2 cells were taken, PBS washed and digested with 0.25% trypsin (25200114, Gibco), blown into individual cells and counted. 500 cells were added into every well of a 6-well plate and cultured for 14 d (Cao *et al.*, 2023). Every 2 to 3 days, the culture medium was refreshed. The culture was terminated when clonal cell clusters were visible to the naked eye. Aspirated the culture solution and rinsed it twice with PBS. Subsequently, the cells were exposed to 4% paraformaldehyde (441244, Sigma-Aldrich) and fixed for 20 min. The fixative was discarded, dyed with crystal violet (C0775, Sigma-Aldrich) for 15 min. Photographed and counted for the number of clone formation using an inverted fluorescence microscope (MF52-N, Guangzhou Ming-Mei Technology Co., Ltd, Guangdong, China).

EdU staining

The proliferation of HepG2 cells was examined with the EdU Cell Proliferation Assay Kit (C0071S, Beyotime). Cells from different treatment groups were cultured for 48 h, then rinsed twice with PBS before being exposed to a 10 μM EdU culture solution for 1 h away from light. Following two PBS rinses, cells were subjected to 4% paraformaldehyde for a duration of 15 min. PBS with 0.3% Triton X-100 (X100, Sigma-Aldrich) was added to permeabilize for 10 min, and incubated with the Click reaction solution in darkness for 30 min. Then, DAPI solution (D9542, Invitrogen) was added and incubated for about 10min and after anti-burst blocking, it was observed and photographed with an inverted fluorescence microscope.

Wound healing assay

HepG2 cells were routinely digested and collected and 1 mL of cell suspension (1×10^6 cells/mL) was aspirated with a sterile lance tip and inoculated into a 6-well plate with the horizontal line drawn in advance. After the cells were fully adhered to the wall and grew to more than 80% density, a vertical line was gently scribed perpendicular to the horizontal line at the base of the 6-well plate using a 20 μL sterile tip (Cao *et al.*, 2023). PBS was washed to remove floating cells and serum-free medium containing BBR or $CoCl_2$ was added. The observation of scratch healing occurred at two time points: 0 h and 48 h. Utilizing Image J software, the widths of scratches were measured to determine the cell migration rate.

Transwell

The Matrigel (354230, Corning, Tewksbury, MA, USA) was thinned out using serum-free DMEM medium, and then 100 μL of the thinned gel was placed in each Transwell chamber (Corning) and left in the incubator overnight. On the next day, the remaining liquid in the chambers was aspirated. HepG2 cell suspension (200 μL) was inoculated into the upper chamber, and 800μL of complete medium containing BBR or $CoCl_2$ was inoculated into the lower chamber, subsequently incubated for 24 h. The matrix gel and cells that had not crossed the membrane were wiped away, then exposed to 4% paraformaldehyde, dyed with 0.1% crystal violet,

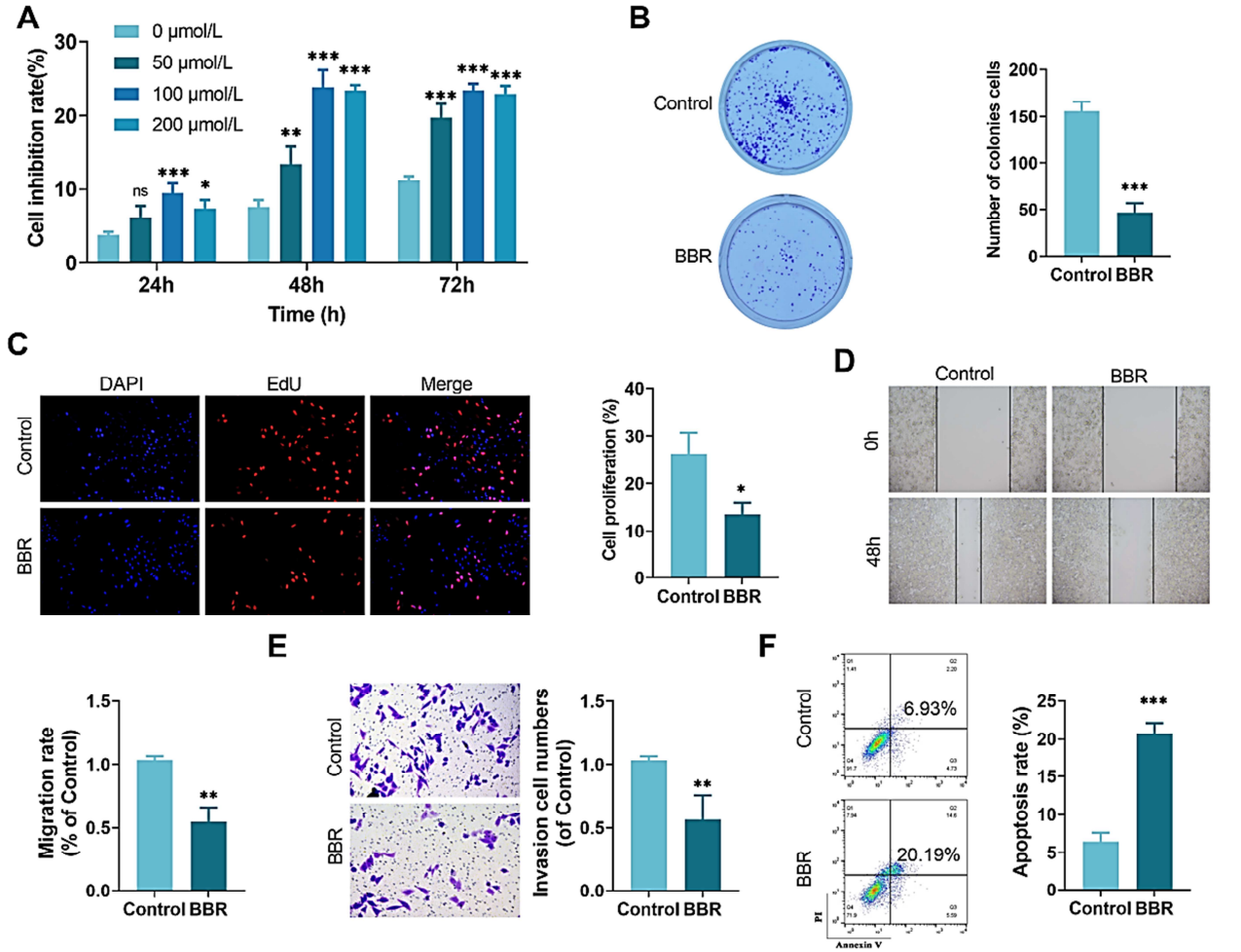

(A) After treatment with different concentrations of BBR (0, 50, 100, or 200 μmol/L) for varying time (24, 48, or 72 h), CCK-8 assay examined the inhibition rate of HepG2 cell proliferation, to determine the most effective concentration and treatment time. (B) Clone formation assay evaluated the effect of 100 μmol/L BBR treatment for 48 h on HepG2 cell proliferation. (C) EDU staining detected the proliferation of HepG2 cells after BBR treatment, with the cell proliferation rate subsequently computed. (D) Wound healing assay assessed cell migration after BBR treatment, with the cell migration rate subsequently computed. (E) Transwell assay assessed cell invasion after BBR treatment, with the cell invasion rate was calculated. (F) Annexin V/PI assay detected the apoptosis rate after BBR treatment. (**P*<0.05, ***P*<0.01, ****P*<0.001 vs Control)

Fig. 1: Effect of BBR on biological processes in HCC cells

subsequently washed twice with PBS (Dai *et al.*, 2020). Randomly selected fields of view in each well were photographed using an inverted fluorescence microscope, and the amount of invasive cells was counted.

Flow cytometry

HepG2 cells were gathered after different treatments, rinsed two times with PBS and gently mixed by adding 500 μL of Binding Buffer. Following that, Annexin-V-FITC (5 μL, HY-K1073, Med Chem Express) and propidium iodide (5 μL, ST1569, Beyotime) were introduced and allowed to incubate for 15 min in darkness (Yu *et al.*, 2022). Sample tubes were used to transfer the samples, and apoptosis was then identified through flow cytometry (BD FACS Calibur TM, BD biosciences, San Jose, CA, USA).

RT-qPCR

The total RNA of HepG2 cells were isolated by Trizol reagent (15596026, Invitrogen)(Fei *et al.*, 2024). Then adding AMV reverse transcriptase (2621, TAKARA, Tokyo, Japan) to obtain the cDNA. Relative levels of mRNA were calculated using the $2^{-\Delta\Delta Ct}$ method. The internal reference used in the analysis was β-actin.

The following primer sequences were utilized in this research: HIF-1α: F: 5'-CTCCCCTTACTCCACCCTGA-3'; R: 5'-TCTTGCTAAGGAACCAAAGTCA-3'. Glucose transporter type 1 (GLUT1): F: 5'-GGAGCAGGTTA CTACAGGGC-3'; R: 5'-ATGGCTCCACCAGGGAAA TG-3'. Hexokinase 2 (HK2): F: 5'-CCTCAGTGAGTGC CTGATCC-3'; R: 5'-ATTTTCCTGGCGCATAGCCT-3'. Lactate dehydrogenase A (LDHA): F: 5'-AAAGGCTAC ACATCCTGGGC-3'; R: 5'-AGCATTCAAATGCAGCG

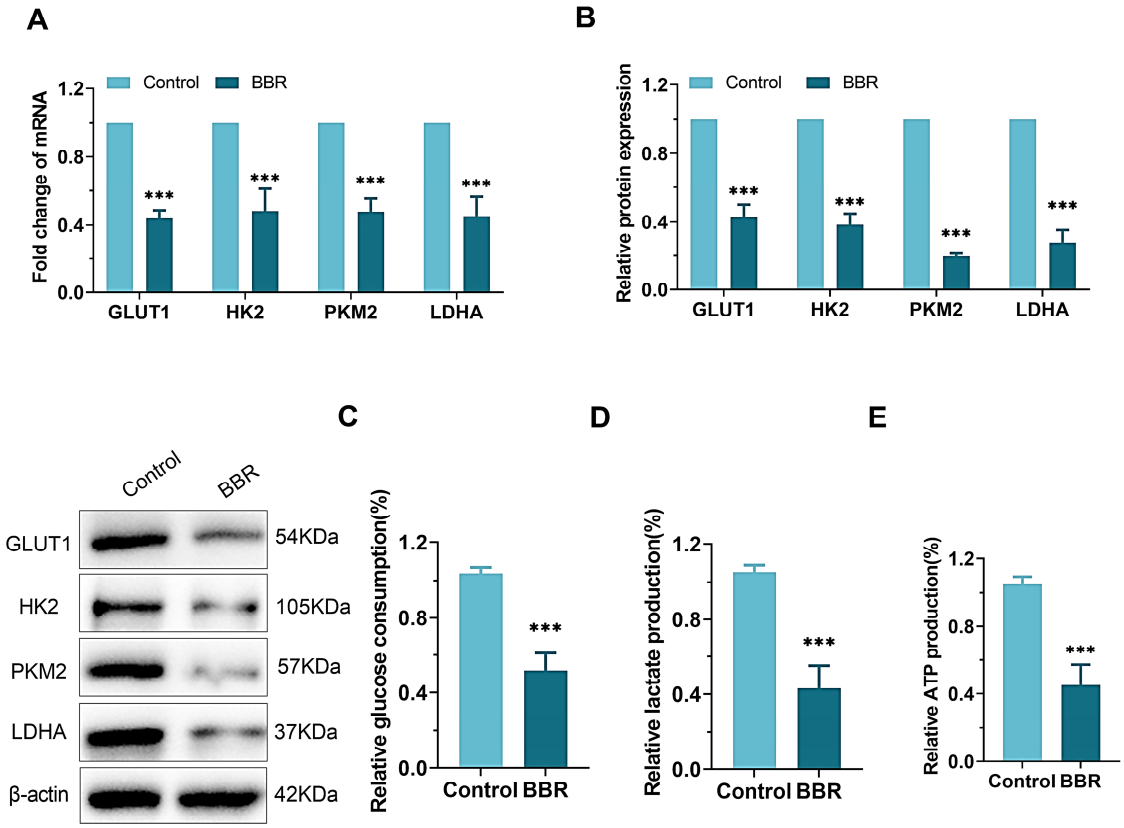

(A) RT-qPCR analyzed the levels of GLUT1, HK2, PKM2, and LDHA mRNA following a 48-hour exposure to 100 μmol/L BBR. (B) Western blot detected the levels of GLUT1, HK2, PKM2 and LDHA proteins. (C-E) Different kits were used to detect glucose consumption, lactate production and ATP production levels in BBR-treated HepG2 cells. (***P<0.001 vs Control)

Fig. 2: Impact of BBR on glycolysis in HCC cells

TATCA-3'. Pyruvate kinase M2 (PKM2): F: 5'-ATGG AGGCGCATTGAGGATT-3'; R: 5'-CGTTCCTTCCAG ATCAGGCG-3'. β-actin: F: 5'-TCCTATGGGAGAACG GCAGA-3'; R: 5'-TCCTTTGTCCCCTGAGCTTG-3'.

Glucose consumption and lactate and Adenosine triphosphate (ATP) production measurements

The concentration of HepG2 cells in 6-well plates was adjusted to 1.0×10^6 cells/well. After various treatments, the glucose levels in the culture medium were assessed through a glucose assay kit (S0201S, Beyotime), the glucose uptake was determined by comparing glucose levels in the control group (Chen *et al.*, 2022). The culture medium was aspirated, lysed the cells, and the supernatant was centrifuged and set aside. Standard curves were plotted and lactate and ATP production in HepG2 cell supernatants were assessed following the guidelines of the Lactate Content Assay Kit (A019-2-1, Nanjing Jiancheng Bioengineering lnstitute, Nanjing, Jiangsu, China) and ATP Assay Kit (S0027, Beyotime).

Subcutaneous tumor model in nude mice

Nude mice have no thymus, are immunocompromised and are commonly used to construct tumour models. Healthy BALB/c nude mice, aged between 4 and 6 weeks, were obtained from Vital river (Beijing, China) and they were kept at a consistent temperature of 22°C with a humidity of 55% to 60%. Each nude mouse was injected subcutaneously in the right axilla with 0.2 mL of logarithmic growth phase HepG2 cell suspension (2×10^6 cells/each) to establish a xenograft tumor model. When the tumor volume reaches approximately 200 mm^3 (Xie *et al.*, 2019), refer to Zhang *et al.* for dosing (Zhang *et al.*, 2020b), the mice were divided into Control (injected with 0.3 mL saline), BBR-1 group (injected with 10 mg/kg BBR) and BBR-2 group (injected with 40 mg/kg BBR) in a random manner, with 5 mice in each group. The drug was administered once a day for 21d of continuous intraperitoneal injection. The size of subcutaneous tumors in nude mice was measured using vernier calipers on d 1, 7, 14 and 21. The mice were then anesthetized and euthanized on day 21 and the tumors were excised and photographed for documentation. Laboratory animals were kept in accordance with national standards for the management of medical laboratory animals and followed the Code of Ethics for Laboratory Animals. The First Affiliated Hospital of Soochow University Experimental Animal Ethics Committee approved this experiment (No. XXX).

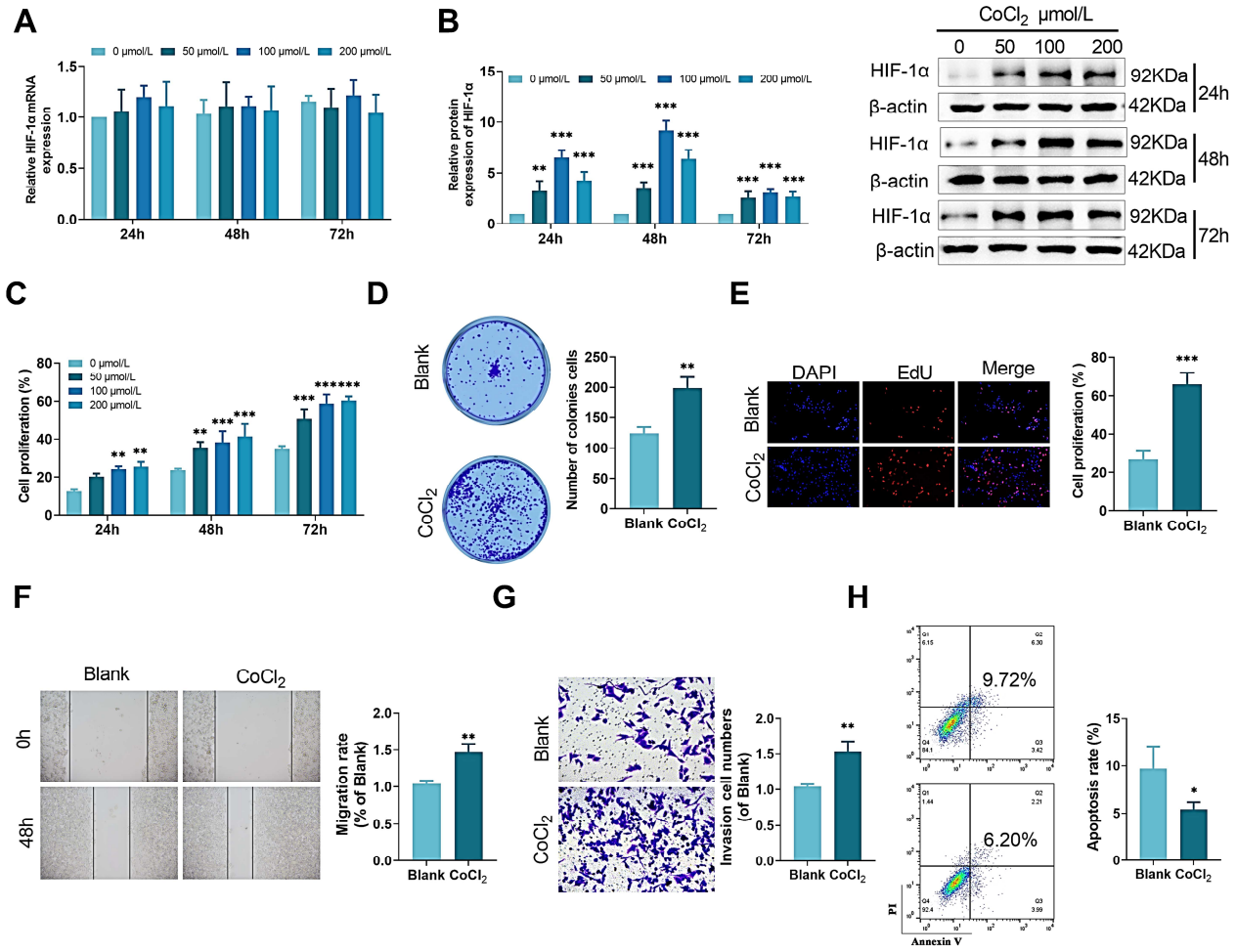

(A) After treatment with $CoCl_2$ (0, 50, 100, or 200 μmol/L) for varying time (24, 48, or 72 h), RT-qPCR quantified the expression of HIF-1α mRNA. (B) Western blot examined the expression of HIF-1α protein after $CoCl_2$ treatment. (C) CCK-8 assay assessed cell proliferation rate after treatment with $CoCl_2$ (0, 50, 100, or 200 μmol/L) for varying time (24, 48, or 72 h). The optimal concentration and treatment time were screened. (D) Clone formation assay evaluated the effect of 100 μmol/L $CoCl_2$ treatment for 48 h on cell proliferative ability. (E) The cell proliferation after $CoCl_2$ treatment was observed by EDU staining. (F) The cell migration after $CoCl_2$ treatment was assessed by wound healing assay. (G) Transwell assay assessed the invasion of HepG2 cells after $CoCl_2$ treatment. (H) Apoptosis rate after $CoCl_2$ treatment was examined by Annexin V/PI method. (*P<0.05, **P<0.01, ***P<0.001 vs Blank)

Fig. 3: Impact of HIF-1α on biological processes in HCC cells

Tunel staining

Nude mice tumor tissues were exposed to 4% paraformaldehyde, routinely dehydrated, sectioned after paraffin embedding (thickness of 4~5 μm) and deparaffinized with xylene (247642, Sigma-Aldrich). Gradient ethanol (100%, 95%, 75% and 50%) hydration for 5 min each. DNase-free proteinase K (20 μg/mL, ST532, Beyotime) slowly introduced and the reaction was performed for 30 min and rinsed twice with PBS. TUNEL assay solution (C1086, Beyotime) was slowly added and left to incubate for 1.5 h away from light (Chen *et al.*, 2022). Then incubated with DAPI staining solution for 10 min. Fluorescence microscopy was used to observe and take pictures.

Immunohistochemistry

Paraffin sections of tumor tissue specimens from nude mice were routinely deparaffinized and microwaved for antigen repair. The samples were exposed to a 3% H_2O_2 solution for 25 min, followed by three washes with PBS. Drops of 5% bovine serum albumin (V900933, Sigma-Aldrich) were added to cover the tissues evenly and closed for 30 min (Dai *et al.*, 2020). Ki67 primary antibody (ab15580, 1:1000, Abcam) was gently added and left to incubate for 90 min. Subsequently, the tissues were covered with HRP-labeled goat anti-rabbit IgG (31460, 1:10000, Invitrogen) and left to incubate for 20 min. DAB (DA1010, Solarbio, Beijing, China) developed the color and tap water terminated the color development. Mayer Hematoxylin (MHS16, Sigma-Aldrich) was re-stained and after neutral gum sealing, observed under an inverted fluorescence microscope.

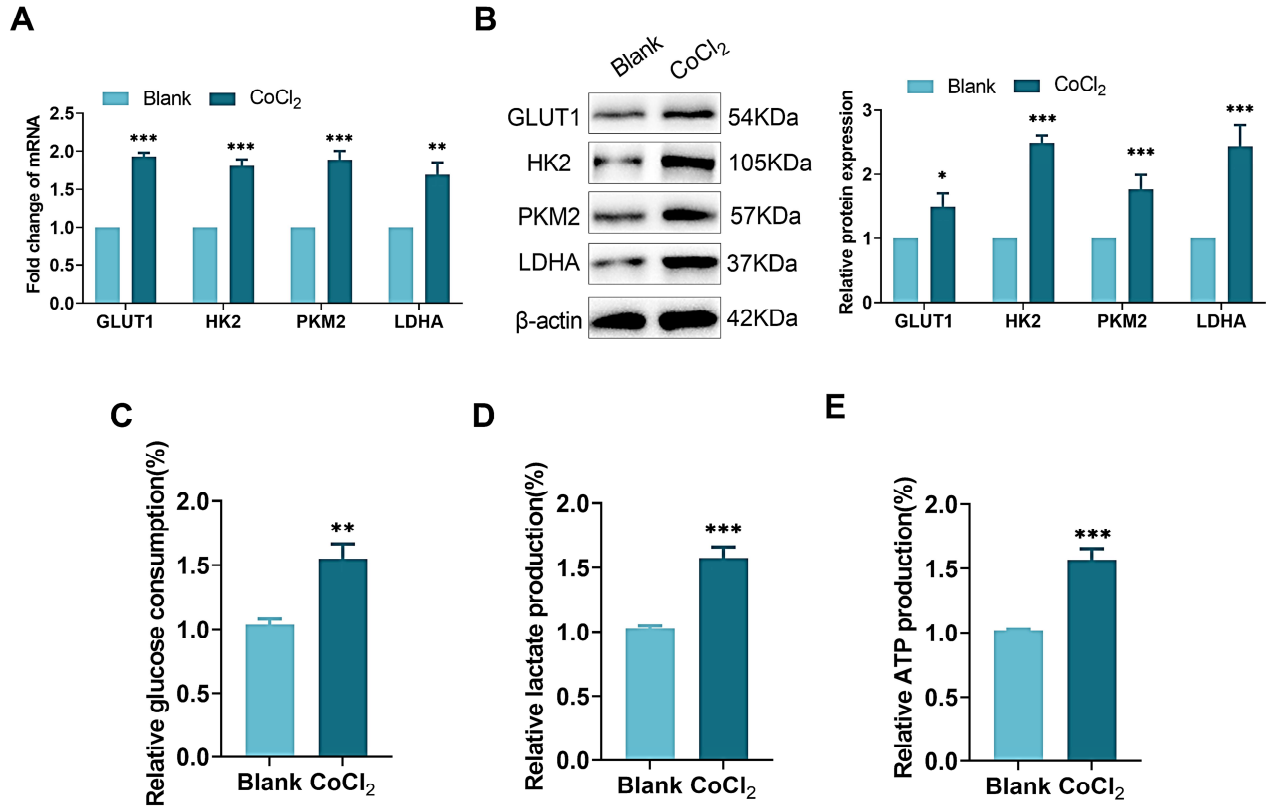

(A) After 48 h of treatment with 100 μmol/L $CoCl_2$, RT-qPCR detected the mRNA levels of GLUT1, HK2, PKM2 and LDHA. (B) Western blot detected the levels of GLUT1, HK2, PKM2 and LDHA protein. (C-E) Different kits were used to detect glucose consumption, lactate production and ATP production levels in HepG2 cells after $CoCl_2$ treatment. (*P<0.05, **P<0.01, ***P<0.001 vs Blank)

Fig. 4: Impact of HIF-1α on glycolysis in HCC cells

Western blot

RIPA lysate (P0013B, Beyotime) was added to different treatment groups of HepG2 cells or tumor tissues and lysed to obtain proteins (Dai *et al.*, 2020). The BCA protein assay kit (P0012, Beyotime) was utilized to assess the protein content. Protein samples underwent electrophoresis on SDS-PAGE gels, followed by move to PVDF membranes (Invitrogen) and sealed for 3 h. After rinsing twice with PBS, the samples were placed at 4°C for an overnight incubation with GLUT1 primary antibody (MA5-31960, 1:5000, Invitrogen), HK2 primary antibody (ab227198, 1:5000, Abcam), PKM2 primary antibody (ab85555, 1:100, Abcam) and LDHA primary antibody (PA5-27406, 1:500, Invitrogen). On the next day, goat anti-rabbit IgG (1:10,000) was incubated for 2 h after washing the membrane 3 times. The chemiluminescent agent ECL (34577, Invitrogen) was evenly dripped onto the membrane and observed using a gel imaging system (WD-9413B, Liuyi Biotechnology Co., Ltd, Beijing, China). The grayscale values of each protein band were obtained after processing the images with Image J software, taking β-actin (MA1-140, 1:5000, Invitrogen) as an internal reference.

Ethical approval

The animal experiment protocol received approval from the Experimental Animal Ethics Committee of the First Affiliated Hospital of Soochow University (No. 2023180).

STATISTICAL ANALYSIS

A minimum of 3 repetitions were performed for each experiment, with the data being reported as mean value with the standard deviation. For statistical analysis of data and image plotting, we employed SPSS 26.0 software (IBM SPSS Statistics 26) and Prism software (Graphpad 9.0). Student's *t*-test evaluated the distinctions between the two groups and one-way ANOVA was applied to make comparisons between sub-multiple groups. * represent a notable contrast in comparison to the Control or Blank groups, and # represents a notable contrast in comparison to the BBR group (P<0.05).

RESULTS

Effect of BBR on biological processes in HCC cells

After treatment with BBR (0, 50, 100, or 200 μmol/L) for 24, 48, or 72 h, the inhibition rate of HepG2 cell

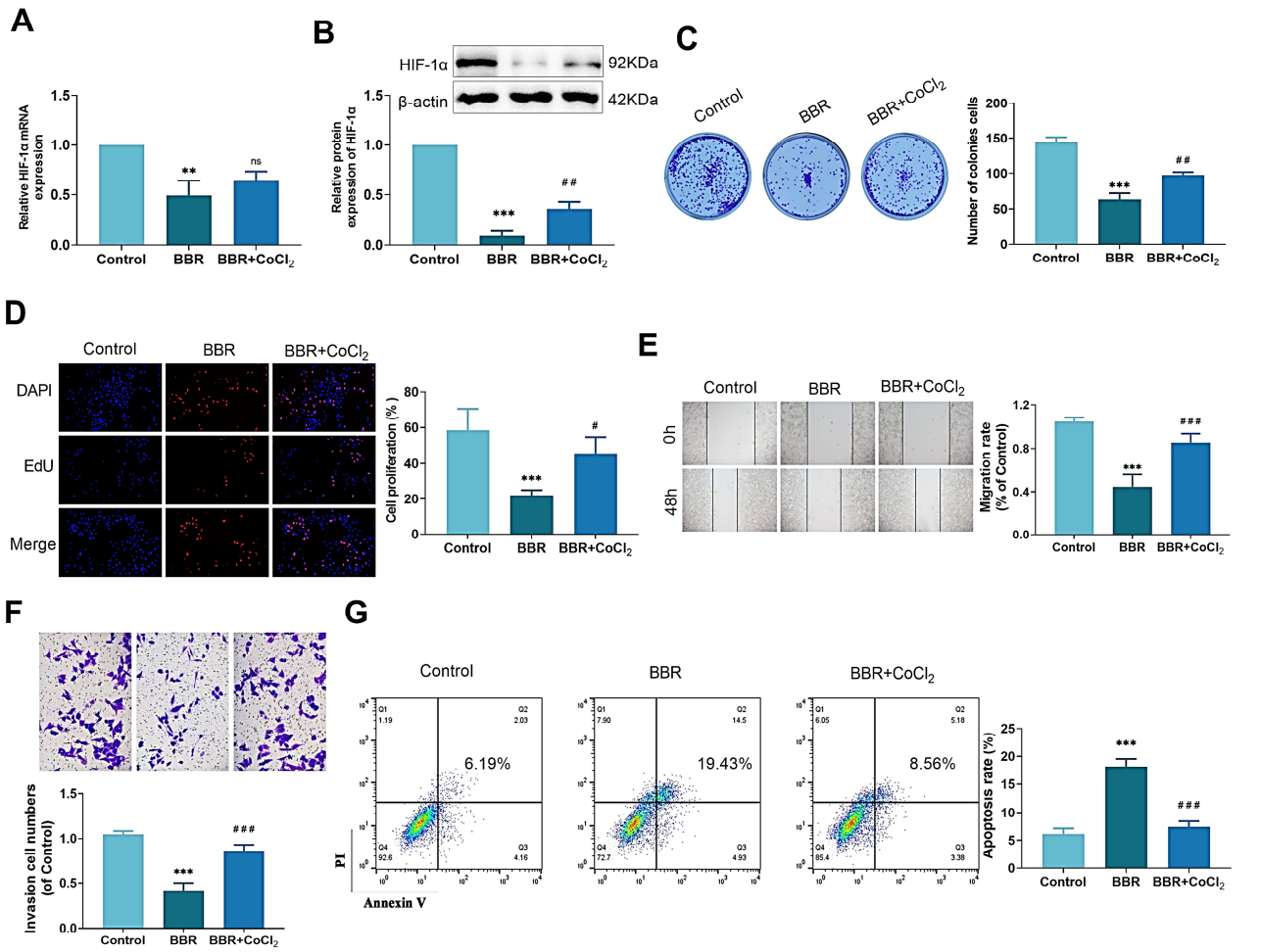

(A) First, 100 μmol/L $CoCl_2$ was added 1 h in advance and then 100 μmol/L BBR was added, and both of them co-treated the cells for 48 h. RT-qPCR quantified the expression of HIF-1α mRNA. (B) After 48 h of $CoCl_2$ and BBR treatment, Western blot detected the level of HIF-1α protein. (C) Clone formation assay assessed the impacts of $CoCl_2$ and BBR treatment on cell proliferative capacity. (D) The proliferation of HepG2 cells after $CoCl_2$ and BBR treatment was observed by EDU staining. (E) Wound healing assay detected cell migration after $CoCl_2$ and BBR treatment. (F) Transwell assay assessed cell invasion after $CoCl_2$ and BBR treatment. (G) Annexin V/PI assay detected the apoptosis rate of HepG2 cells after $CoCl_2$ and BBR treatment. (**P<0.01, ***P<0.001 vs Control; ns P>0.05, #P<0.05, ## P<0.01, ###P<0.001 vs BBR)

Fig. 5: BBR exerts inhibitory effect on HCC cell progression by regulating the HIF-1α expression

proliferation was examined by the CCK-8 assay. The findings indicated that treating HepG2 cells with 100 μmol/L BBR for 48 hours caused the greatest suppression of cell proliferation (fig. 1A). Thus, we chose BBR (100 μmol/L) treatment for 48 h as the cell culture condition for subsequent experiments. The number of clone formation in HepG2 cells was notably reduced after BBR treatment, as shown in the clone formation assay (fig. 1B). After treatment with BBR, the amount of EDU-positive cells was notably declined, as detected by EDU staining, suggesting that BBR effectively suppressed cell proliferation (fig. 1C). Wound healing assay results revealed that BBR treatment caused a marked decline in migration rate (fig. 1D). Transwell results indicated that after BBR treatment, the cell invasion rate was markedly reduced (fig. 1E). Not only that, flow cytometry results indicated that BBR treatment caused a significantly higher apoptosis rate in HepG2 cells (fig. 1F). The above findings demonstrated that BBR treatment suppressed the proliferation, invasion and migration and induced apoptosis of HepG2 cells.

Impact of BBR on glycolysis in HCC cells

To explore the influence of BBR on glycolysis in HepG2 cells, we detected the levels of glycolysis-associated proteins. RT-qPCR findings demonstrated that after treatment with 100μmol/L BBR for 48 h, the levels of GLUT1, HK2, PKM2, and LDHA mRNA were markedly reduced in HepG2 cells (fig. 2A). Western blot assay results similarly showed that treating HepG2 cells with BBR caused a notable reduction in the levels of GLUT1, HK2, PKM2 and LDHA (fig. 2B). Next, we used

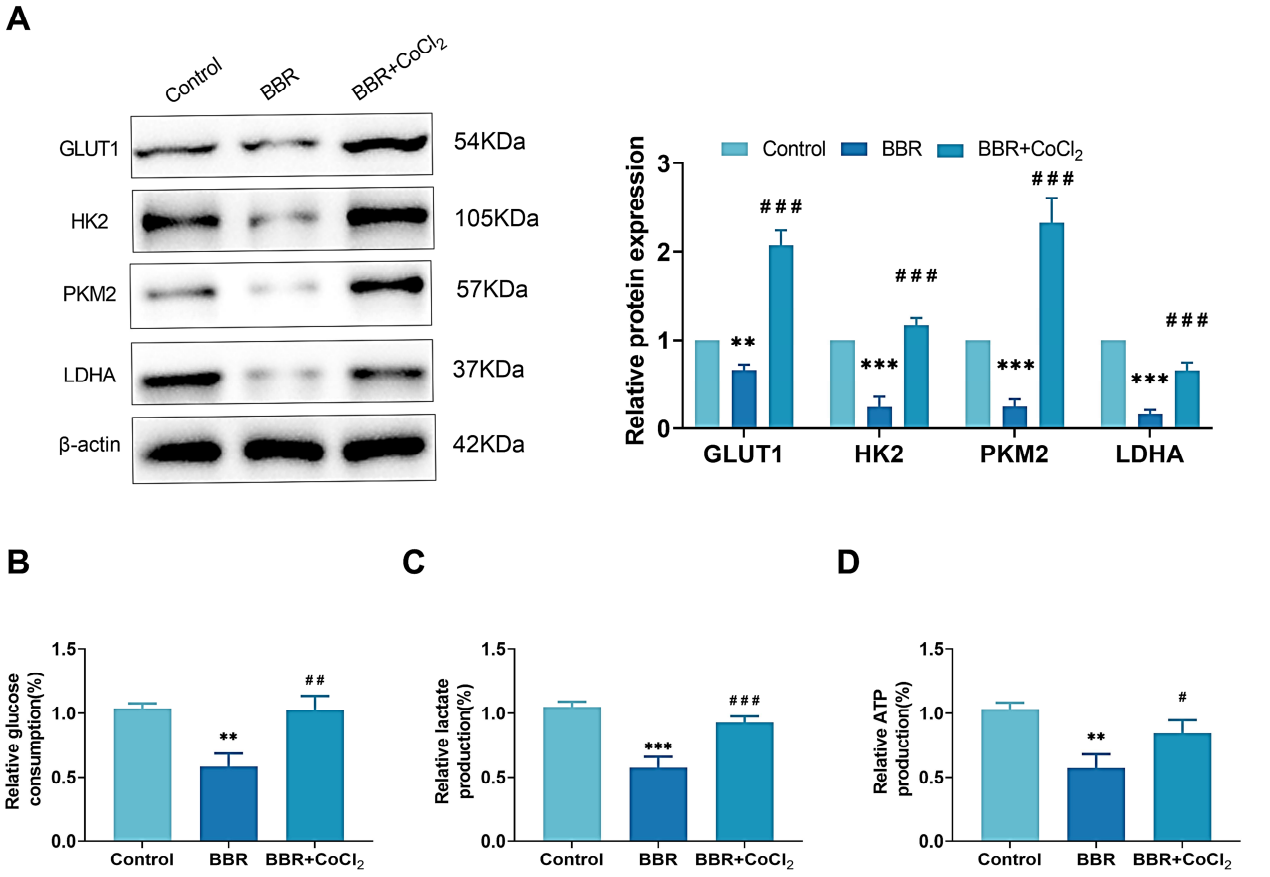

(A) After 48 h of $CoCl_2$ and BBR treatment, Western blot detected the levels of GLUT1, HK2, PKM2 and LDHA proteins. (B-D) Different kits were used to detect glucose consumption, lactate production and ATP production levels after $CoCl_2$ and BBR treatment. (***P*<0.01, ****P*<0.001 vs Control; #*P*<0.05, ## *P*<0.01, ###*P*<0.001 vs BBR)

Fig. 6: BBR exerts inhibitory effect on glycolysis in HCC cells by regulating the HIF-1α expression

different kits to detect glucose consumption and lactate and ATP production. The results revealed that BBR treatment caused a significant decrease in glucose consumption (fig. 2C) and a significant decrease in lactate and ATP production (fig. 2D-2E) in HepG2 cells, suggesting that BBR inhibits the glycolytic process in HepG2 cells.

Effects of HIF-1α on biological processes in HCC cells

Next, we used $CoCl_2$ to mimic the hypoxic TME *in vitro* with HepG2 cells. After treatment with $CoCl_2$ (0, 50, 100, or 200 μmol/L) for 24, 48, or 72 h, the level of HIF-1α mRNA was unaffected (fig. 3A). Notably, HIF-1α protein level in HepG2 cells was notably elevated with $CoCl_2$ treatment, suggesting that hypoxia impacts the level of HIF-1α expression (fig. 3B). After $CoCl_2$ treatment, cell proliferation rate was significantly increased and the influence was dose-dependent and time-dependent (fig. 3C). Therefore, combining the results of the above experiments, we chose to treat HepG2 cells with 100 μmol/L $CoCl_2$ for 48 h. $CoCl_2$ treatment increased the number of clone formation (fig. 3D) and the amount of EDU-positive cells (fig. 3E), indicating that elevated HIF-1α expression promotes cell proliferation. Not only that, $CoCl_2$ treatment resulted in significantly higher migration rate (fig. 3F) and invasion rate (fig. 3G) of HepG2 cells, suggesting that elevated HIF-1α promotes cell migration and invasion. Additionally, flow cytometry results demonstrated that after $CoCl_2$ treatment, the apoptosis rate was markedly reduced (fig. 3H). These results demonstrated that HIF-1α level was elevated in the hypoxic HepG2 cell model induced by $CoCl_2$, leading to increased proliferation, migration and invasion and reduced apoptosis.

Effect of HIF-1α on glycolysis in HCC cells

Following a 48-hour treatment with 100μmol/L $CoCl_2$, there was a marked increase in the levels of GLUT1, HK2, PKM2 and LDHA mRNA in HepG2 cells (fig. 4A). Western blot findings similarly demonstrated that the levels of GLUT1, HK2, PKM2 and LDHA protein were notably increased after $CoCl_2$ treatment (fig. 4B). Not only that, we used different kits to detect the impacts of $CoCl_2$ treatment on glucose consumption and lactate and ATP production. The results showed that $CoCl_2$ treatment resulted in significantly higher glucose consumption (fig.

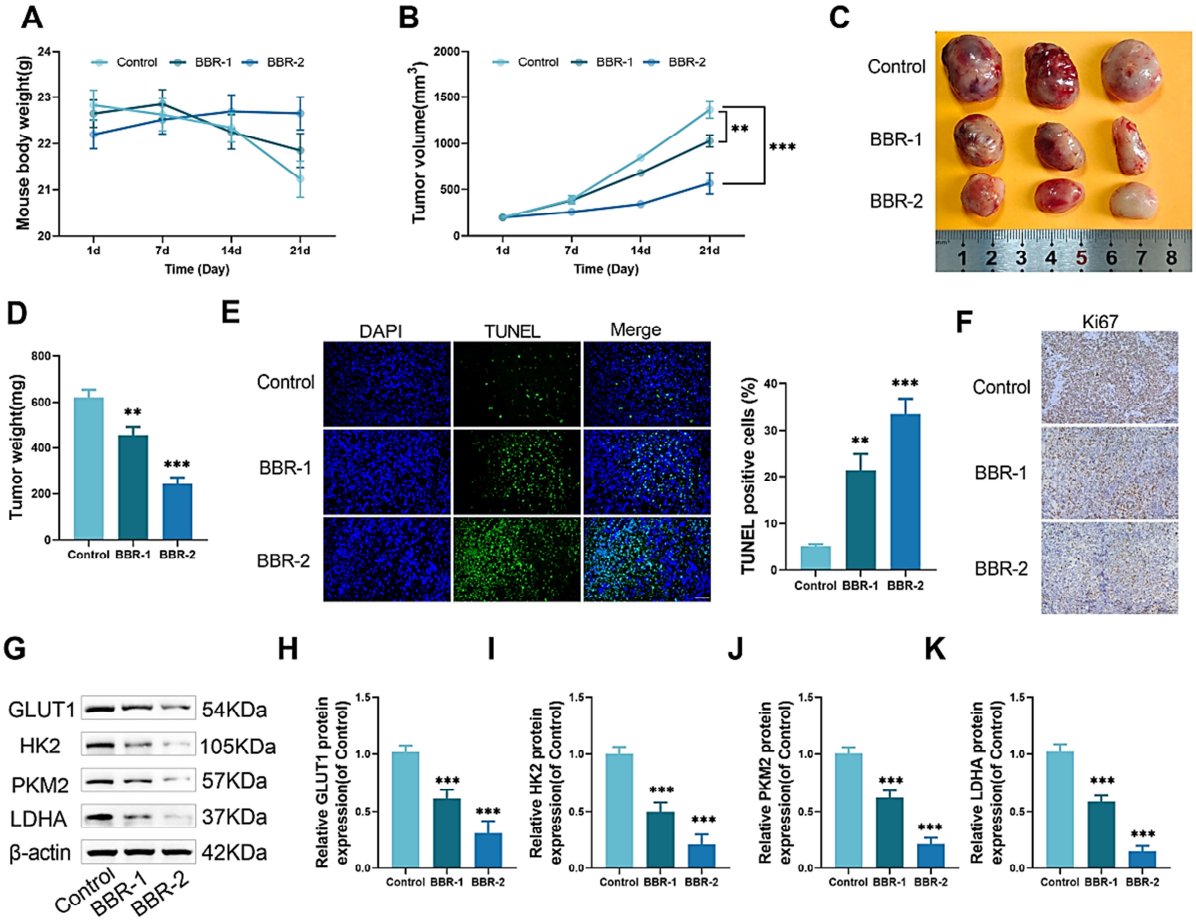

Nude mice were injected subcutaneously with HepG2 cell suspension, when the tumor volume reaches approximately 200 mm^3, the mice were divided into Control group (0.3 mL saline), BBR-1 group (10 mg/kg BBR) and BBR-2 group (40 mg/kg BBR) in a random manner. Administration is by intraperitoneal injection, once a day for 21 d. Mice were weighed at 1, 7, 14 and 21 d (A) and the size of subcutaneous tumors in nude mice was measured with vernier calipers to calculate tumor volume (B). On d 21, nude mice were executed after anesthesia, tumors were excised, photographed for documentation (C) and weighed (D). (E) Tunel staining detected apoptosis in tumor tissues and quantified the rate of Tunel-positive cells. (F) Immunohistochemical determined Ki-67 expression in tumor tissues. (G-K) Examining the levels of GLUT1(H), HK2(I), PKM2(J) and LDHA(K) in tumor tissues through Western blot. (**P<0.01, ***P<0.001 vs Control)

Fig. 7: BBR inhibits proliferation and glycolysis of HCC cells *in vivo*.

4C) and significantly higher lactate and ATP production (fig. 4D-4E), indicating that elevated levels of HIF-1α enhanced glycolysis in HepG2 cells.

BBR exerts inhibitory effect of BBR on HCC cell progression by regulating the HIF-1α expression

To determine whether BBR inhibits the malignant behaviors of HepG2 cells by modulating the level of HIF-1α, cells were treated with $CoCl_2$ and BBR together. The RT-qPCR findings demonstrated that treatment with BBR caused a notable decline in the mRNA level of HIF-1α, with the presence of $CoCl_2$ showing no significant impact on the influence of BBR (fig. 5A). BBR markedly declined the protein level of HIF-1α, whereas $CoCl_2$ weakened the effect of BBR, which further confirmed that hypoxia regulates HIF-1α expression at the protein level (fig. 5B). Additionally, BBR treatment decreased the number of clone formation (fig. 5C) and EDU-positive cells (fig. 5D), whereas $CoCl_2$ weakened the inhibitory impact of BBR on cell proliferation. BBR treatment caused a significant decrease in migration rate (fig. 5E) and invasion rate (fig. 5F), and the addition of $CoCl_2$ attenuated the effects of BBR. Not only that, after BBR treatment, the apoptosis rate was increased, whereas the addition of $CoCl_2$ caused a significant decrease in apoptosis rate (fig. 5G). The above results indicated that $CoCl_2$ intervention weakened the inhibition of BBR on the malignant progression of HepG2 cells, suggesting that BBR exerts its cancer inhibitory effect by regulating HIF-1α expression.

BBR exerts inhibitory impact of BBR on glycolysis in HCC cells

Next, we explored whether BBR inhibited the glycolytic process in HepG2 cells by regulating HIF-1α expression. Western blot results demonstrated that after treated with

BBR, HepG2 cells exhibited a notable decline in the levels of GLUT1, HK2, PKM2 and LDHA, however, $CoCl_2$ intervention attenuated the effect of BBR treatment (fig. 6A). In addition, our research revealed that BBR treatment notably reduced glucose consumption, and lactate and ATP production in HepG2 cells, whereas $CoCl_2$ intervention resulted in significantly higher glucose consumption, lactate and ATP production (fig. 6B-6D). These results further indicated that $CoCl_2$ intervention attenuated the inhibitory impact of BBR on glycolysis, suggesting that BBR exerts its inhibitory effect on glycolysis by modulating HIF-1α expression.

BBR inhibits proliferation and glycolysis of HCC cells in vivo

Finally, we found an overall decreasing trend in body weight in the control mice, an increase and then a decrease in the BBR-1 group, and an overall increasing trend in the BBR-2 group (fig. 7A). The volume and weight of tumors were notably declined after BBR injection, and the higher the concentration, the better the effect (figs. 7B-7D). By TUNEL staining, we noticed a significant rise in the amount of TUNEL-positive cells with BBR treatment, indicating that BBR enhanced the apoptosis of HCC cells (fig. 7E). We used immunohistochemistry to detect the level of Ki67 and the findings indicated that the level of Ki67 was markedly reduced after injection of BBR, which indicated that BBR inhibited cell proliferation (fig. 7F). In addition, BBR treatment inhibited glycolysis in tumor tissues, leading to a notable decrease in the levels of GLUT1, HK2, PKM2 and LDHA (fig. 7G-7K). These results further indicated that BBR was able to trigger apoptosis and impede proliferation and glycolysis of HCC cells *in vivo*.

DISCUSSION

HCC has an insidious and aggressive onset, patients with HCC in the US experience an average five-year survival rate of 19.6%, making it one of the deadliest malignant tumors (Piñero *et al.*, 2020, Chidambaranathan-Reghupaty *et al.*, 2021). Therefore, finding novel and efficient drugs to inhibit the progression of HCC is crucial for improving the prognosis of HCC patients. BBR, the primary active compound found in *Coptis chinensis*, has been a hot spot in the research of natural anticancer drugs in recent years (Habtemariam, 2020, Rauf *et al.*, 2021). Research has revealed that BBR can effectively hinder gastric cancer cell proliferation and trigger cell autophagy and apoptosis (Zhang *et al.*, 2020b). Vishnoi *et al*. found that BBR dose-dependently reduced HCC cell viability by inhibiting β-Catenin signaling, resulting in cell cycle arrest and mitochondrial damage (Vishnoi *et al.*, 2021). Adiditionally, BBR enhances the effects of anti-tumour drugs. It is reported that BBR enhance BBR enhances gemcitabine toxicity to bladder cancer cells (Gao *et al.*, 2022), and can improve the inhibitory effect of gefitinib on epithelial mesenchymal transition in lung cancer cells (Zheng *et al.*, 2020). In this study, we screened the optimal concentration and time of BBR treatment of HCC cells by CCK-8 assay, and found that treating HepG2 cells with BBR (100 μmol/L) for 48 h caused the most notable inhibition of cell proliferation. Additionally, BBR treatment hindered cell invasion and migration, and stimulated apoptosis both *in vivo* and *in vitro*, confirming the potential of BBR for the management of HCC.

Many research investigations have indicated that HIF-1α is linked to tumor angiogenesis and drug resistance, as well as the promotion of metastasis and invasion of cancer cells, highlighting its significance as a target for tumor therapy (Rashid *et al.*, 2021, Ashrafizadeh, 2024, Zhao *et al.*, 2024). High levels of HIF-1α are commonly found in the tumor tissues of the majority of HCC patients, this elevated expression is linked to lower overall survival rates and a heightened likelihood of postoperative recurrence (Wada *et al.*, 2006, Xiao *et al.*, 2014). Wang *et al*. discovered that the protein level of HIF-1α was elevated in the tumor hypoxic microenvironment, which in turn promoted HCC metastasis (Wang *et al.*, 2023). Therefore, we used $CoCl_2$ treatment of HepG2 cells to mimic the tumor hypoxic microenvironment to induce HIF-1α expression (Jiang *et al.*, 2020). Notably, HIF-1α mRNA level remained unaffected by $CoCl_2$ treatment, while HIF-1α protein level was notably increased. Specifically, the relative level of HIF-1α protein in HepG2 cells was increased from 1 to 9.17 after treatment with 100 μmol/L $CoCl_2$ for 48 h. A similar phenomenon was found by Lin *et al*, HIF-1α mRNA level did not exhibit significantly change under hypoxic and normoxic conditions, but HIF-1α protein level showed a notable increase in hypoxic conditions (Lin *et al.*, 2022). Next, our study revealed that treating HCC cells with $CoCl_2$ stimulated their proliferation, invasion and migration and also suppressing apoptosis.

The life activities of cells are inseparable from the supply of energy. The production of ATP through glycolysis is important for the constant growth and spread of cancer cells, serving as a vital energy source for tumor cells (Chelakkot *et al.*, 2023). Normal cells use oxidative phosphorylation of glucose in mitochondria as the primary energy supply. In contrast, tumor cells exhibit a preference for converting glucose to lactate, even in the presence of oxygen. This metabolic shift is marked by a significant rise in glucose consumption and lactate generation (Abbaszadeh *et al.*, 2020, Paul *et al.*, 2022). In the process of cancer cells to glycolysis, HIF-1α mediates the up-regulation of glycolytic enzymes such as LDHA, HK2, PKM2 and phosphoglycerol kinase 1, as well as glucose and lactate transport proteins like GLUT1 and monocarboxylic acid transporter protein 4 levels, to enhance glucose uptake (Kierans and Taylor, 2021, Vaupel *et al.*, 2021). Our study confirmed that BBR treatment reduced GLUT1, HK2, PKM2 and LDHA levels and glucose consumption, lactate and ATP

production levels, suggesting that BBR can effectively inhibit glycolysis. In contrast, $CoCl_2$ treatment was able to up-regulate glycolysis-related proteins and increase glucose consumption, lactate and ATP production levels, confirming that HIF-1α mediates the glycolytic process in HepG2 cells.

To deeply investigate whether BBR inhibits the malignant progression of HCC and the glycolytic process by regulating HIF-1α expression, we first intervened HepG2 cells with $CoCl_2$ and then added BBR to co-treat the cells. We found that BBR treatment did not impact HIF-1α mRNA level, but it successfully decreased HIF-1α protein level, indicating that BBR suppressed HIF-1α expression. Zeng *et al*. similarly found that BBR reduced HIF-1α levels under hypoxic and low-glucose conditions in cervical cancer cells (Zeng *et al.*, 2020). A bioinformatics analysis and molecular docking results showed that BBR and HIF-1α protein can bind to each other, and the absolute value of the binding energy is greater than 5 kcal/mol, indicating that it has strong binding activity (Li *et al.*, 2024). Notably, $CoCl_2$ intervention weakened the inhibition of BBR on the proliferation, migration, invasion and glycolysis process of HepG2 cells, confirming that BBR inhibited the malignant progression and glycolysis of HCC through down-regulating HIF-1α expression.

CONCLUSION

BBR treatment inhibits malignant biological progression and glycolytic processes in HCC cells. Highly expressed HIF-1α promotes malignant biological progression and glycolytic processes in HCC cells and impairs the anti-tumor effect of BBR, while BBR treatment down-regulates the expression of HIF-1α. Therefore, BBR may play an anti-tumor role through down-regulating HIF-1α expression. This research provides a reliable reference for targeted therapy and drug screening in HCC. However, there are some limitations in this research, further assessment is required in the future to determine the safety and effectiveness of BBR in clinical settings. We have focused on the fact that BBR can regulate HIF-1α expression, but the regulation of BBR on other cancer-promoting genes remains to be elucidated. In addition, anticancer drugs can be developed targeting BBR in the future.

REFERENCES

Abbaszadeh Z, Çeşmeli S and Biray Avcı C (2020). Crucial players in glycolysis: Cancer progress. *Gene* **726**: 144158.

Ashrafizadeh M (2024). Cell death mechanisms in human cancers: Molecular pathways, therapy resistance and therapeutic perspective. *J. Can. Biomol. Therap.,* **1**(1): 17-40.

Cao M, Ren Y, Li Y, Deng J, Su X, Tang Y, Yuan F, Deng H, Yang G, He Z, Liu B, Yao Z and Deng M (2023). Lnc-ZEB2-19 inhibits the progression and lenvatinib resistance of hepatocellular carcinoma by attenuating the NF-κB signaling pathway through the TRA2A/RSPH14 axis. *Int. J. Biol. Sci.,* **19**(12): 3678-3693.

Chelakkot C, Chelakkot VS, Shin Y and Song K (2023). Modulating glycolysis to improve cancer therapy. *Int. J. Mol. Sci.,* **24**(3): 2606.

Chen K, Li Y, Wang B, Yan X, Tao Y, Song W, Xi Z, He K and Xia Q (2023). Patient-derived models facilitate precision medicine in liver cancer by remodeling cell-matrix interaction. *Front. Immunol.,* **14**: 1101324.

Chen Y, Jiang Y, Huang X, Chen L, Yang H, Zhao J and Liang B (2022). Cordycepin inhibits the growth of hepatocellular carcinoma by regulating the pathway of aerobic glycolysis. *Evid. Based Complement. Alternat. Med.,* 6454482.

Chidambaranathan-Reghupaty S, Fisher PB and Sarkar D (2021). Hepatocellular carcinoma (HCC): Epidemiology, etiology and molecular classification. *Adv. Cancer Res.,* **149**: 1-61.

Cogliati B, Yashaswini CN, Wang S, Sia D and Friedman SL (2023). Friend or foe? The elusive role of hepatic stellate cells in liver cancer. *Nat. Rev. Gastroenterol. Hepatol.,* **20**(10): 647-661.

Dai H, Li M, Yang W, Sun X, Wang P, Wang X, Su J, Wang X, Hu X and Zhao M (2020). Resveratrol inhibits the malignant progression of hepatocellular carcinoma via MARCH1-induced regulation of PTEN/AKT signaling. *Aging (Albany N.Y.)* **12**(12): 11717-11731.

Fei M, Li X, Liang S, Zhou S, Wu H, Sun L, Liu Y, Hu Q, Liu L and Wang J (2024). LncRNA PWRN1 inhibits the progression of hepatocellular carcinoma by activating PKM2 activity. *Cancer Lett.,* **584**: 216620.

Feng J, Li J, Wu L, Yu Q, Ji J, Wu J, Dai W and Guo C (2020). Emerging roles and the regulation of aerobic glycolysis in hepatocellular carcinoma. *J. Exp. Clin. Cancer Res.,* **39**(1): 126.

Gao X, Liu J, Fan D, Li X, Fang Z, Yan K and Fan Y (2022). Berberine enhances gemcitabine-induced cytotoxicity in bladder cancer by downregulating Rad51 expression through inactivating the PI3K/Akt pathway. *Oncol. Rep.,* **47**(2): 33.

Habtemariam S (2020). Berberine pharmacology and the gut micro biota: A hidden therapeutic link. *Pharmacol. Res.,* **155**: 104722.

Hassanipour S, Vali M, Gaffari-Fam S, Nikbakht HA, Abdzadeh E, Joukar F, Pourshams A, Shafaghi A, Malakoutikhah M, Arab-Zozani M, Salehiniya H and Mansour-Ghanaei F (2020). The survival rate of hepatocellular carcinoma in Asian countries: A systematic review and meta-analysis. *EXCLI J.,* **19**: 108-130.

Hinshaw DC and Shevde LA (2019). The tumor microenvironment innately modulates cancer progression. *Cancer Res.,* **79**(18): 4557-4566.

Huang R, Zhang L, Jin J, Zhou Y, Zhang H, Lv C, Lu D, Wu Y, Zhang H, Liu S, Chen H, Luan X and Zhang W (2021). Bruceine D inhibits HIF-1α-mediated glucose metabolism in hepatocellular carcinoma by blocking ICAT/β-catenin interaction. *Acta Pharma. Sini. B.,* **11**(11): 3481-3492.

Jampasri S, Reabroi S, Tungmunnithum D, Parichatikanond W and Pinthong D (2022). Plumbagin suppresses breast cancer progression by downregulating HIF-1α expression via a PI3K/Akt/mTOR independent pathway under hypoxic condition. *Molecules.,* **27**(17): 5716.

Jiang N, Zhao H, Han Y, Li L, Xiong S, Zeng L, Xiao Y, Wei L, Xiong X, Gao P, Yang M, Liu Y and Sun L (2020). HIF-1α ameliorates tubular injury in diabetic nephropathy via HO-1-mediated control of mitochondrial dynamics. *Cell Prolif.,* **53**(11): e12909.

Kheshtchin N and Hadjati J (2022). Targeting hypoxia and hypoxia-inducible factor-1 in the tumor microenvironment for optimal cancer immunotherapy. *J. Cell Physiol*., **237**(2): 1285-1298.

Kierans SJ and Taylor CT (2021). Regulation of glycolysis by the hypoxia-inducible factor (HIF): implications for cellular physiology. *J. Physiol.* **599**(1): 23-37.

Kim E and Viatour P (2020). Hepatocellular carcinoma: old friends and new tricks. *Exp. Mol. Med.,* **52**(12): 1898-1907.

Li J, Dan W, Zhang C, Liu N, Wang Y, Liu J and Zhang S (2024). Exploration of berberine against ulcerative colitis via TLR4/NF-κB/HIF-1α pathway by bioinformatics and experimental validation. *Drug Des. Devel. Ther.,* **18**: 2847-2868.

Lin Y and Guo L (2022). GLI1 is involved in HIF-1α-induced migration, invasion, and epithelial-mesenchymal transition in glioma cells. *Folia Histochem Cytobiol.,* **60**(2): 156-166.

Liu L, Fan J, Ai G, Liu J, Luo N, Li C and Cheng Z (2019). Berberine in combination with cisplatin induces necroptosis and apoptosis in ovarian cancer cells. *Biol. Res.,* **52**(1): 37.

Liu Z, Liu X, Liang J, Liu Y, Hou X, Zhang M, Li Y and Jiang X (2021). Immunotherapy for hepatocellular carcinoma: Current status and future prospects. *Front. Immunol.,* **12**: 765101.

Och A, Podgórski R and Nowak R (2020). Biological activity of berberine-A summary update. *Toxins (Basel).,* **12**(11): 713.

Paul S, Ghosh S and Kumar S (2022). Tumor glycolysis, an essential sweet tooth of tumor cells. *Semin. Cancer Biol.,* **86**(Pt 3): 1216-1230.

Piñero F, Dirchwolf M and Pessoa MG (2020). Biomarkers in hepatocellular carcinoma: Diagnosis, prognosis and treatment response assessment. *Cells* **9**(6): 1370.

Rashid M, Zadeh LR, Baradaran B, Molavi O, Ghesmati Z, Sabzichi M and Ramezani F (2021). Up-down regulation of HIF-1α in cancer progression. *Gene,* **798**: 145796.

Rauf A, Abu-Izneid T, Khalil AA, Imran M, Shah ZA, Emran TB, Mitra S, Khan Z, Alhumaydhi FA, Aljohani ASM, Khan I, Rahman MM, Jeandet P and Gondal T A (2021). Berberine as a potential anticancer agent: A comprehensive review. *Molecules,* **26**(23): 7368.

Rumgay H, Arnold M, Ferlay J, Lesi O, Cabasag CJ, Vignat J, Laversanne M, McGlynn KA and Soerjomataram I (2022). Global burden of primary liver cancer in 2020 and predictions to 2040. *J. Hepatol.* **77**(6): 1598-1606.

Sarcognato S, Sacchi D, Fassan M, Fabris L, Cadamuro M, Zanus G, Cataldo I, Capelli P, Baciorri F, Cacciatore M and Guido M (2021). Cholangiocarcinoma. *Pathologica* **113**(3): 158-169.

Song D, Hao J and Fan D (2020). Biological properties and clinical applications of berberine. *Front. Med.* **14**(5): 564-582.

Sun K, Wu L, Wang S and Deng W (2022). Antitumor effects of Chinese herbal medicine compounds and their nano-formulations on regulating the immune system microenvironment. *Front. Oncol.,* **12**: 949332.

Sun Y, Zhou Q, Chen F, Gao X, Yang L, Jin X, Wink M, Sharopov FS and Sethi G (2023). Berberine inhibits breast carcinoma proliferation and metastasis under hypoxic microenvironment involving gut microbiota and endogenous metabolites. *Pharmacol. Res.,* **193**: 106817.

Sung H, Ferlay J, Siegel RL, Laversanne M, Soerjomataram I, Jemal A and Bray F (2021). Global cancer statistics 2020: GLOBOCAN estimates of incidence and mortality worldwide for 36 cancers in 185 countries. *CA Cancer J. Clin.,* **71**(3): 209-249.

Vaupel P and Multhoff G (2021). Revisiting the Warburg effect: Historical dogma versus current understanding. *J. Physiol.,* **599**(6): 1745-1757.

Vishnoi K, Ke R, Saini KS, Viswakarma N, Nair RS, Das, S, Chen Z, Rana A and Rana B (2021). Berberine represses β-Catenin translation involving 4E-BPs in hepatocellular carcinoma cells. *Mol. Pharmacol.,* **99**(1): 1-16.

Wada H, Nagano H, Yamamoto H, Yang Y, Kondo M, Ota H, Nakamura M, Yoshioka S, Kato H, Damdinsuren B, Tang D, Marubashi S, Miyamoto A, Takeda Y, Umeshita K, Nakamori S, Sakon M, Dono K, Wakasa K and Monden M (2006). Expression pattern of angiogenic factors and prognosis after hepatic resection in hepatocellular carcinoma: Importance of angiopoietin-2 and hypoxia-induced factor-1 alpha. *Liver Int.,* **26**(4): 414-423.

Wang K, Chen Q, Shao Y, Yin S, Liu C, Liu Y, Wang R, Wang T, Qiu Y and Yu H (2021). Anticancer activities

of TCM and their active components against tumor metastasis. *Biomed. Pharmacother.,* **133**: 111044.

Wang Y, Yang Y, Yang Y, Dang Y, Guo Z, Zhuang Q, Zheng X, Wang F, Cheng N, Liu X, Guo W and Zhao B (2023). Hypoxia induces hepatocellular carcinoma metastasis via the HIF-1α/METTL16/lnc-CSMD1-7/RBFOX2 axis. *iScience,* **26**(12): 108495.

Xiao H, Tong R, Cheng S, Lv Z, Ding C, Du C, Xie H, Zhou L, Wu J and Zheng S (2014). BAG3 and HIF-1 α coexpression detected by immunohistochemistry correlated with prognosis in hepatocellular carcinoma after liver transplantation. *BioMed. Res. Int.,* 516518.

Xiao Y and Yu D (2021). Tumor microenvironment as a therapeutic target in cancer. *Pharmacol. Ther.,* **221**: 107753.

Xie L, Dai H, Li M, Yang W, Yu G, Wang X, Wang P, Liu W, Hu X and Zhao M (2019). MARCH1 encourages tumour progression of hepatocellular carcinoma via regulation of PI3K-AKT-β-catenin pathways. *J. Cell. Mol. Med.,* **23**(5): 3386-3401.

Xiong RG, Huang SY, Wu SX, Zhou DD, Yang ZJ, Saimaiti A, Zhao CN, Shang A, Zhang YJ, Gan RY and Li HB (2022). Anticancer effects and mechanisms of berberine from medicinal herbs: An update review. *Molecules,* **27**(14): 4523.

Xu M, Ren L, Fan J, Huang L, Zhou L, Li X and Ye X (2022). Berberine inhibits gastric cancer development and progression by regulating the JAK2/STAT3 pathway and downregulating IL-6. *Life Sci.,* **290**: 120266.

Yu Q, Dai W, Ji J, Wu L, Feng J, Li J, Zheng Y, Li Y, Cheng Z, Zhang J, Wu J, Xu X and Guo C (2022). Sodium butyrate inhibits aerobic glycolysis of hepatocellular carcinoma cells via the c-myc/hexokinase 2 pathway. *J. Cell. Mol. Med.,* **26**(10): 3031-3045.

Zeng X, Wan L, Wang Y, Xue J, Yang H and Zhu Y (2020). Effect of low dose of berberine on the radioresistance of cervical cancer cells via a PI3K/HIF-1 pathway under nutrient-deprived conditions. *Int. J. Radiat. Biol.,* **96**(8): 1060-1067.

Zhang L, Wu X, Yang R, Chen F, Liao Y, Zhu Z, Wu Z, Sun X and Wang L (2020a). Effects of berberine on the gastrointestinal microbiota. *Front. Cell Infect. Microbiol.,* **10**: 588517.

Zhang Q, Wang X, Cao S, Sun Y, He X, Jiang B, Yu Y, Duan J, Qiu F and Kang N (2020b). Berberine represses human gastric cancer cell growth *in vitro* and *in vivo* by inducing cytostatic autophagy via inhibition of MAPK/mTOR/p70S6K and Akt signaling pathways. *Biomed. Pharmacother.,* **128**: 110245.

Zhao Y, Xing C, Deng Y, Ye C and Peng H (2024). HIF-1α signaling: Essential roles in tumorigenesis and implications in targeted therapies. *Genes Dis.,* **11**(1): 234-251.

Zheng F, Li J, Ma C, Tang X, Tang Q, Wu J, Chai X, Xie J, Yang XB and Hann SS (2020). Novel regulation of miR-34a-5p and HOTAIR by the combination of berberine and gefitinib leading to inhibition of EMT in human lung cancer. *J. Cell. Mol. Med.,* **24**(10): 5578-5592.